Simultaneous repetition-rate multiplication and envelope control based on periodic phase-only and phase-mostly line-by-line pulse shaping

José Caraquitena,[1,2,*] Zhi Jiang,[1] Daniel E. Leaird,[1] and Andrew M. Weiner[1]

[1]*School of Electrical and Computer Engineering, Purdue University, 465 Northwestern Avenue, West Lafayette, Indiana 47907-2035, USA*

[2]*Now with Nanophotonics Technology Center, Universidad Politécnica de Valencia, Valencia 46022, Spain*

**Corresponding author: jcaraqui@ntc.upv.es*

Received July 23, 2007; revised September 25, 2007; accepted September 25, 2007; posted October 2, 2007 (Doc. ID 85506); published November 26, 2007

We experimentally demonstrate simultaneous pulse repetition-rate multiplication and periodic pulse-to-pulse peak-intensity control based on optimized periodic spectral line-by-line pulse shaping. Accordingly, the method allows us to generate multiplied pulse trains in which the amplitude of each single pulse in a period can be arbitrarily tailored. The technique is illustrated with the generation of 4×9 GHz arbitrary periodic pulse trains, including binary code patterns, from a 9 GHz uniform input pulse train. Special attention is paid to pulse train generation based on all-pass line-by-line filters. © 2007 Optical Society of America

OCIS codes: 320.5540, 320.7160, 070.6020.

1. INTRODUCTION

Pulse repetition-rate multiplication based on linear spectral filtering constitutes a well-established method for the generation of periodic pulse trains at high repetition rates from a lower rate source. On the one hand, the amplitude-only filtering approach can be interpreted as a mode-selection process: in the frequency domain, mode-locked lasers are described by a series of discrete spectral lines or modes (optical frequency comb) with frequency spacing equal to the pulse repetition rate. By using a periodic amplitude spectral filter with a free spectral range equal to a multiple integer of the input repetition rate, an output pulse train with an increased repetition frequency is obtained. The filter periodically selects a subset of spectral lines, suppressing the other modes located in between. In practice, this technique was originally implemented by using a Fabry–Perot interferometer [1]. Other options have been considered including superstructure fiber Bragg gratings [2]. In this technique, a strong suppression of unwanted modes is critical to generate output trains with minimum peak-to-peak pulse intensity variations. In this way, a double-pass Fabry–Perot configuration [3] and the use of a semiconductor optical amplifier [4] have been proposed to produce uniform pulse trains with a multiplied repetition rate. On the other hand, the phase-only filtering approach has usually been explained in terms of the temporal Talbot effect [5]. This phenomenon occurs when periodic trains of optical pulses propagate through a first-order dispersive medium. An appropriate amount of dispersion leads either to the reproduction of the original pulse train (the integer temporal Talbot effect) or repetition-rate multiplication by an integer factor (the fractional temporal Talbot effect). This option has been traditionally demonstrated by using conventional optical fibers [6,7] or linearly chirped fiber Bragg gratings [8]. When the dispersion deviates from that given by the so-called Talbot condition [5], degradations of the multiplied pulse trains are observed [5,6]. Alternatively, we have demonstrated high-quality tunable pulse repetition-rate multiplication by the temporal Talbot effect implemented via spectral line-by-line pulse shaping [9].

The application of these filtering techniques is limited to the generation of multiplied uniform pulse trains. However, for many applications, including ultrahigh-speed optical communications [10] and the photonically assisted generation of millimeter-wave and microwave electromagnetic waveforms [11], it is desirable to generate high repetition-rate pulse trains with additional control on the amplitude of each pulse. McKinney *et al.* [11] used a direct space-to-time pulse shaper to obtain tailored optical pulse sequences for the subsequent generation of arbitrarily shaped millimeter-wave electromagnetic waveforms. On the other hand, recently the use of spectrally periodic optical filters was proposed for arbitrary periodic pulse train generation from a lower rate pulse source [12]. In the output train, the pulse-intensity profile as well as the pulse width are preserved. In general, pulse-to-pulse phase variations are found in the multiplied train. Lattice-form Mach–Zehnder interferometers have been proposed [12] to achieve arbitrary pulse train generation via amplitude-and-phase spectrally periodic filtering. The optimization of the device parameters was based on a simulated annealing algorithm. Using this approach, the generation of binary code patterns has been demonstrated [13]. However, imperfections in the device fabrication results in output pulse trains with significant degradations.

In this paper, as an extension of our previous work on spectral line-by-line pulse shaping for Talbot-based pulse

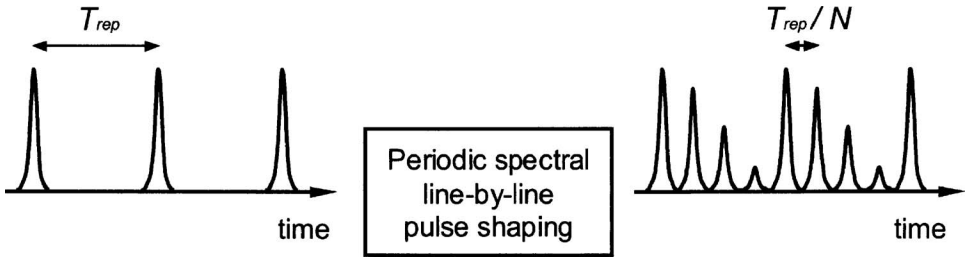

Fig. 1. Schematic of simultaneous repetition-rate multiplication and pulse peak-power control based on spectrally periodic line-by-line pulse shaping.

repetition-rate multiplication, we propose and experimentally demonstrate programmable arbitrary pulse train generation from a lower rate input train. In Section 2, we introduce the optimization algorithm used to design the spectral line-by-line filters that produce simultaneous repetition-rate multiplication and arbitrary pulse-intensity control. In Section 3, the experimental setup is described and the generation of a variety of periodic pulse trains is reported. Finally, in Section 4 we finish the paper with the main conclusions.

2. DESIGN OF SPECTRALLY PERIODIC LINE-BY-LINE FILTERS

As mentioned in Section 1, repetition-rate multiplication with additional periodic pulse modulation can be achieved via spectrally periodic filtering [12]. Our proposal is to perform periodic line-by-line pulse shaping to generate arbitrary pulse trains with a multiplied repetition rate; see Fig. 1. Spectral line-by-line manipulation is implemented by well-developed ultrashort pulse-shaping techniques [14] with a Fourier-transform pulse shaper that incorporates a liquid-crystal modulator (LCM) array to independently control both the amplitude and phase of the individual spectral lines of an optical frequency comb. More details about the line-by-line pulse shaper will be given in Section 3. In this implementation, the parameters to be found are the amplitudes and phases imposed by the line-by-line pulse shaper to each spectral line. For simplicity and high energy efficiency, initially phase-only filtering will be considered. However, phase+amplitude filtering will be also applied when the phase-only filtering approach leads to output pulse trains with inaccurate modulation. We design the filters by using an optimization approach based on a genetic algorithm [15], which has proved to be powerful in other ultrafast optics pulse shaping applications including the control of nonlinear pulse propagation in optical fibers [16,17] and adaptive pulse compression [18]. The algorithm starts from a number of individuals which, in this particular problem, are randomly generated line-by-line periodic filters. These filters constitute the initial population. For a given periodic line-by-line filter, each period is described by a set of N phases and N amplitudes, $\{\phi_1,\phi_2,\ldots,\phi_N\}$ and $\{\kappa_1,\kappa_2,\ldots,\kappa_N\}$, respectively. In our filter design algorithm, we assume that the integer N coincides with the multiplication factor of the output pulse train. Maximum repetition-rate multiplication is limited by the input pulse duration, which must be short enough to prevent pulse overlapping in the multiplied train. The population update is based on the evaluation of a cost or fitness function that we define as

$$F=\sum_{i=1}^{N}|I^i_{\text{peak}}-I^i_{\text{peak,target}}|, \tag{1}$$

where I^i_{peak} is the peak power of the pulse i in the multiplied train and $I^i_{\text{peak,target}}$ is the desired peak power for that pulse. Note that only N pulses are involved in this function as the output pulse train is constituted by an N-pulse sequence that is repeated periodically, as shown in Fig. 1. The goal is to find the filter that minimizes the fitness function. The ideal solution is reached when $F=0$, i.e., when the output pulse train is exactly the target. First, the fitness function of every individual is evaluated and some individuals are selected, based on their fitness-function value, and modified, based on crossover and mutation operators, to create a new generation of individuals. Then, this new population is used in the next iteration (generation) of the algorithm. The process is repeated until a given fitness-function value, or a predetermined number of iterations, is reached. As an example, let us consider the generation of a 4×9 GHz periodic sequence, with a pulse peak-intensity pattern $[1,1,0.5,0.5]$, from a 9 GHz input pulse train with a Gaussian pulse shape of full-width-half-maximum 4.5 ps. As four-times repetition-rate multiplication is pursued, the periodic line-by-line filter to be designed is completely characterized by four different spectral phases $\{\phi_1,\phi_2,\phi_3,\phi_4\}$ and amplitudes $\{\kappa_1,\kappa_2,\kappa_3,\kappa_4\}$. Our filter design method is particularized to phase-only line-by-line filters so that $\kappa_i=1$ for $i=1,\ldots,4$. As we will show in Section 3, the phase-only approach is good enough to successfully generate a wide variety of pulse trains. After applying the genetic algorithm, with a population of 200 individuals and 200 generations, we obtain an optimum spectral line-by-line phase filter with phases $\{0,0.749\pi,0.156\pi,1.905\pi\}$. The fitness-function value for this optimized filter is $F=1.7\times 10^{-3}$. Figure 2(a) shows the input pulse spectrum together with the line-by-line phase-only filter. In Fig. 2(b), the input pulse train is depicted. Figure 2(c) shows the corresponding four-times multiplied output pulse train obtained by numerical simulation. As expected, in each period, the peak intensity of two pulses is reduced by 50% compared with uniform pulse repetition-rate multiplication. Note that the output train exhibits a pulse-to-pulse phase variation.

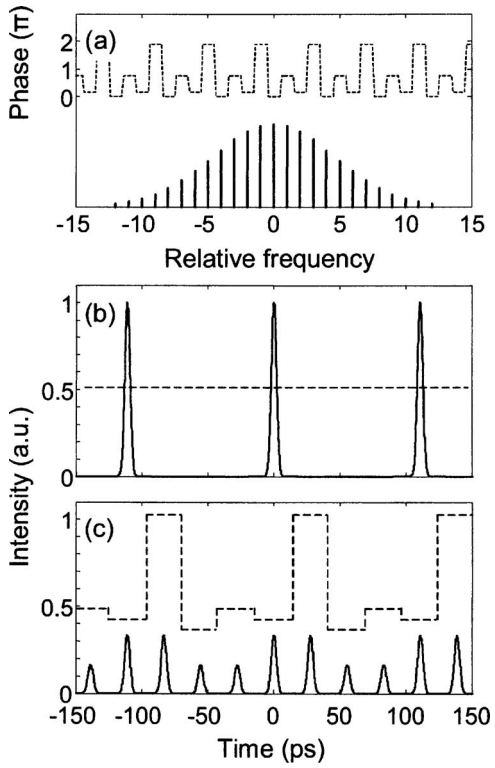

Fig. 2. (a) Input pulse spectrum together with the line-by-line phase-only filter (dashed curve). (b) Input pulse train at 9 GHz. (c) Four-times multiplied pulse train obtained via optimized periodic line-by-line pulse shaping. The pulse peak-power profile in each period is [1,1,0.5,0.5]. The phases of the any four consecutive pulses are different (dashed curve).

3. EXPERIMENTAL SETUP AND RESULTS

A home-built harmonically mode-locked Er-fiber laser producing ~4 ps pulses at a ~9 GHz repetition rate is the pulse source. The discrete spectral lines of the mode-locked laser are manipulated by a fiber coupled Fourier-transform pulse shaper in a reflective geometry. The resulting optical signal is characterized by using an optical spectrum analyzer with 0.01 nm resolution and a 50 GHz photodiode followed by a sampling oscilloscope with 50 GHz bandwidth. Intensity cross-correlation measurements are also performed. Our line-by-line pulse shaper is described in detail in [19]. Briefly, the shaper comprises an ~18 mm diameter input beam, a 1200 grooves/mm diffraction grating, a 1000 mm focal length lens, an LCM array with a 12.8 mm aperture and 2×128 independent pixels, a retroreflecting mirror, and a circulator. A fiberized polarization controller is used to adjust horizontal polarization on the grating. The LCM, with a polarizer on the input face just before the lens focal plane, allows us to independently control both the amplitude and phase of individual spectral lines. The fiber-to-fiber insertion loss is 11.6 dB (including circulator loss). The passband width, measured by scanning a tunable, narrow-linewidth, continuous-wave laser with the LCM replaced by a narrow slit, is 2.6 GHz at the 3 dB points. The spectral dispersion of the pulse shaper is designed such that the spacing between adjacent spectral lines corresponds to precisely two LCM pixels. The pulse shaper is adjusted for zero chromatic dispersion [14]; hence, negligible broadening is observed when input pulses pass through the pulse shaper without spectral filtering.

In most of the examples we will show in this section, a phase-only approach is considered that has proved to be suitable for the generation of a wide variety of pulse trains with high fidelity. We emphasize that the use of all-pass filters has some advantages, compared with amplitude-only or amplitude-and-phase filters, including high energy efficiency. On the other hand, our experiments are based on four-times repetition-rate multiplication so that four-pulse periodic sequences are generated. All the pulse sequences are normalized to the maximum peak-power value. As a first example, we consider the generation of a pulse train with peak-power profile [1,1,0.5,0.5], previously introduced in Section 2. Figure 3(a) shows the intensity cross correlation of the input pulse train at 9 GHz. In Fig. 3(b) we show the output pulse train when the LCM in the line-by-line pulse shaper is programmed to apply the optimized phase filter obtained by the genetic algorithm. As expected, a 36 GHz pulse train is generated. All pulses have the same intensity profile and pulse width, which coincide with those of the input pulses. However, the peak power of two consecutive pulses is reduced by a factor of 2. We must mention that, for this case and the other examples shown here, initially we found some deviations between the experimental peak-power profiles and the expected results from the optimized filters. These discrepancies are attributed to small errors in the calibration of the LCM and to weak cross talk between adjacent spectral lines due to finite spectral resolution. Then, to generate pulse trains with correct modulations, small changes in the applied phase shifts are necessary. We use an iterative correction algo-

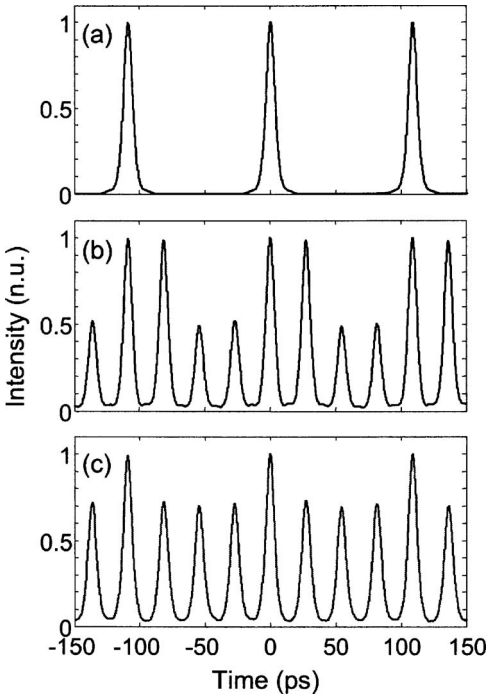

Fig. 3. Generation of two-value periodic pulse sequences. (a) Intensity cross-correlation trace of the input pulse train. (b), (c) Measured cross-correlations of the pulse sequences with peak-power patterns [1,1,0.5,0.5] and [1,0.7,0.7,0.7], respectively.

Table 1. Optimized Phase-Only Line-by-Line Filters Leading to User-Defined Four-Times Multiplied Periodic Pulse Patterns[a]

Periodic Pattern	Optimized Line-by-Line Phase-Only Filter [π]	Fitness-Function Value (from Simulation)	Fitness-Function Value (from Experiment)
[1,1,0.5,0.5]	{0,0.749,0.156,1.905}	1.7×10^{-3}	4.4×10^{-2}
[1,0.7,0.7,0.7]	{0,0,0,0.799}	0.3×10^{-3}	4.0×10^{-2}
[1,1,1,0]	{0,1.515,0.407,1.892}	2.4×10^{-3}	2.7×10^{-2}
[1,0,2/3,1/3]	{0,0.435,0.268,0.705}	3.8×10^{-3}	4.2×10^{-2}
[1,0.8,0.6,0.4]	{0,1.969,1.273,0.077}	3.3×10^{-3}	2.5×10^{-2}

[a]The corresponding fitness-function values are also given.

rithm that adaptively modifies the phases applied by the LCM until the output train is close to the target. The correction algorithm is based on fast oscilloscope measurements. A similar procedure was used to equalize the multiplied pulse trains generated via the temporal Talbot effect [9]. Oscilloscope detection often induces some distortion in the output trains. Then, in general, a second minor phase correction is required to obtain optimum results when intensity cross-correlation measurements are considered. As cross-correlation measurements are slow compared with fast oscilloscope detection, in this second correction, phase changes are based on cross correlations performed only for discrete delays, which coincide with pulse peak-power locations. The rms (maximum) spectral phase change imposed by the algorithm for the different examples shown in this paper was 0.058 rad (0.152 rad). As a second example, we generated the two-value periodic sequence [1,0.7,0.7,0.7]. The output pulse train obtained after performing line-by-line pulse shaping is shown in Fig. 3(c). The optimized periodic phase-only filter that generates this pattern is given in Table 1 together with the optimized filters found for the following examples. In addition, the corresponding fitness-function values are also included, both numerical and experimental.

As particular relevant examples of two-value periodic pulse trains, we now focus our interest on the generation of pulse sequences with binary code profiles. This sort of pulse train is particularly attractive for optical communications applications. Figures 4(a) and 4(b) show the generation of the pulse trains with modulations [1,1,1,0] and [1,1,1,1], respectively. In the first case, the missing pulse has been successfully suppressed. In both cases, note the high uniformity of the pulses so that binary patterns are generated with high fidelity. Note that the phase-only filter that generates multiplied uniform pulses is obtained from the Talbot condition [5,9] with indices $s=1$ and $r=4$. As another example, we consider the binary pulse sequence [1,1,0,0]. In Fig. 5(a) we show the resultant pulse train obtained after applying the optimized phase-only filter, given in Table 2, with the line-by-line pulse shaper. As desired, an equalized doublet is generated in each period. Note, however, the partial suppression of the missing pulses. Specifically, ~81% suppression is achieved for both pulses, relative to the peak power of the other pulses in the periodic sequence. This value is consistent with the theoretical ~83% suppression found in the output train obtained by numerical simulation. Accordingly, a significantly worse fitness-function value is obtained compared with the previous examples. The measured output optical spectrum is also shown, which is very similar to the input spectrum, see the figure inset, confirming that a phase-only filtering process is performed. In order to generate the binary pulse sequence [1,1,0,0] with more fidelity, a combined amplitude-and-phase filtering approach must be employed. First, a "phase-mostly" approach is considered. In particular, the optimization algorithm is constrained to provide filters with normalized amplitudes higher than 0.707, i.e., with a 50% maximum intensity attenuation for each spectral line. Figure 5(b) shows the resultant cross-correlation trace and the corresponding optical spectrum, obtained after performing combined amplitude-and-phase line-by-line pulse shaping. Now, the peak power of the undesired pulses has been reduced to ~6% and 7% compared with the peak power of the other two pulses in each period. Numerical simulation results predict peak-power values ~4% and 6%, respectively, which agree very well with the experimental results. The amplitude contribution of the applied filter translates into the attenuation of some spectral lines in the measured optical spectrum, as shown in the figure. We have also applied the optimization algorithm without any constraint on the optimized filter and a specific amplitude-and-phase filter has been found. As a result, the output depicted in Fig. 5(c) is generated. By applying this filter, the suppression of the missing pulses has been improved. In particular, 1.6% and 1.2% peak

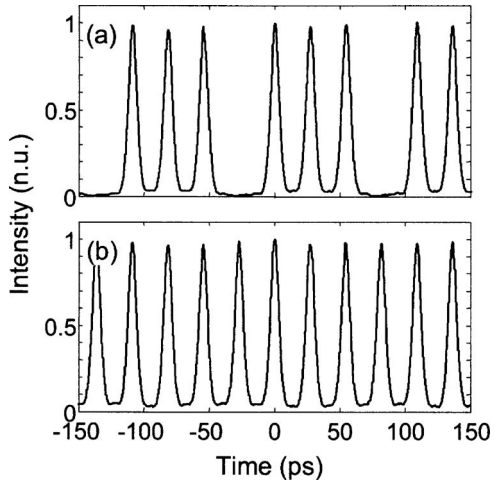

Fig. 4. Generation of binary code pulse sequences. (a), (b) Measured intensity cross correlations of the pulse sequences with peak-power patterns [1,1,1,0] and [1,1,1,1], respectively.

Table 2. Generation of the Periodic Pattern [1,1,0,0] with Phase-Only, Phase-Mostly, and Phase+Amplitude Periodic Filtering

Optimized Line-by-Line Filter {Amplitude}+{Phase [π]}		Fitness-Function Value (from Simulation)	Fitness-Function Value (from Experiment)
{1,1,1,1}	{0,1.747,0.497,0.250}	3.44×10^{-1}	3.77×10^{-1}
{0.707,1,1,0.707}	{0,1.784,1.515,1.262}	1.05×10^{-1}	1.28×10^{-1}
{0.535,1,0.873,0.223}	{0,1.729,1.493,1.243}	0.02×10^{-1}	0.32×10^{-1}

powers are obtained. We point out that the use of an optimization algorithm is unnecessary to find a periodic phase+amplitude filter leading to pulse train multiplication and modulation. In this way, the algorithm provides an alternative amplitude-and-phase filter leading to the same modulation.

Finally, we analyze the generation of more complex four-times multiplied pulse trains with arbitrary peak-power variations. In particular, Figs. 6(a) and 6(b) show intensity cross-correlation measurements of the pulse trains with peak-power patterns [1,0,2/3,1/3] and [1,0.8,0.6,0.4], respectively, obtained by phase-only filtering. For these examples and all the previously reported experimental results we find less than 3% deviations between the resultant pulse peak powers and the theoretical modulations provided by the optimized filters, which is confirmed by the experimental fitness-function values.

4. CONCLUSIONS

In summary, we have demonstrated a technique for programmable pulse repetition-rate multiplication with ad-

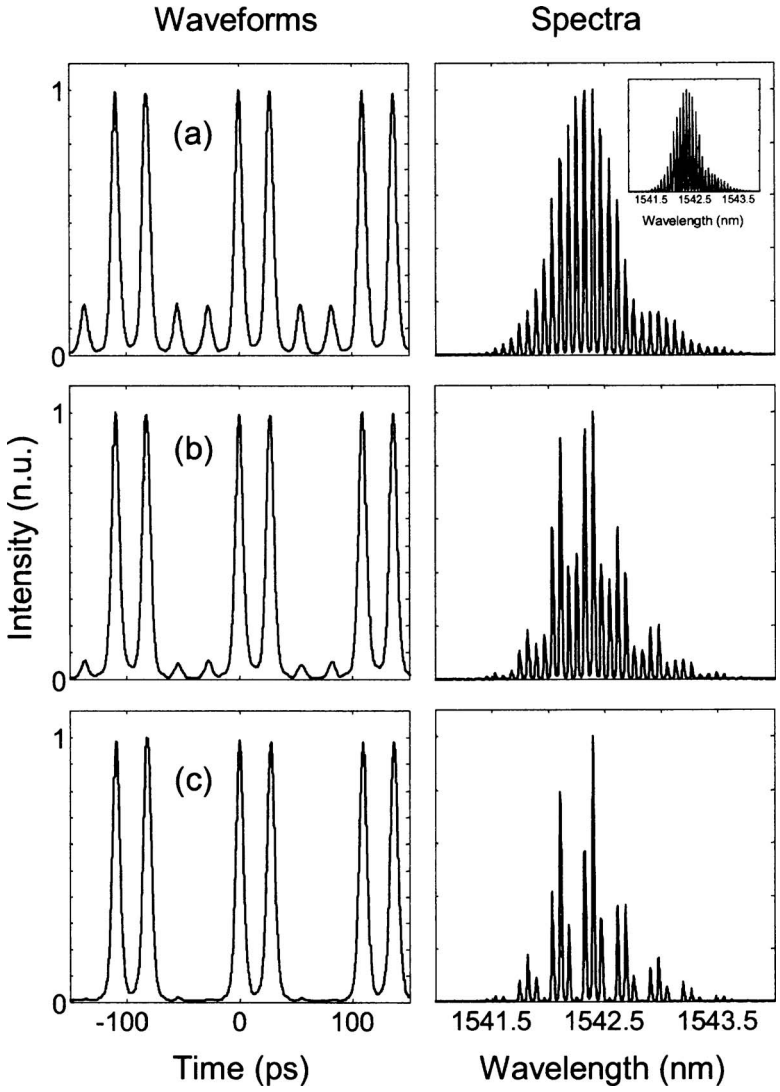

Fig. 5. Measured intensity cross-correlation traces of the binary code pulse sequence [1,1,0,0] generated with (a) phase-only, (b) phase-mostly, and (c) phase+amplitude line-by-line pulse shaping. The corresponding normalized optical spectra are also shown. Inset figure shows the input optical spectrum.

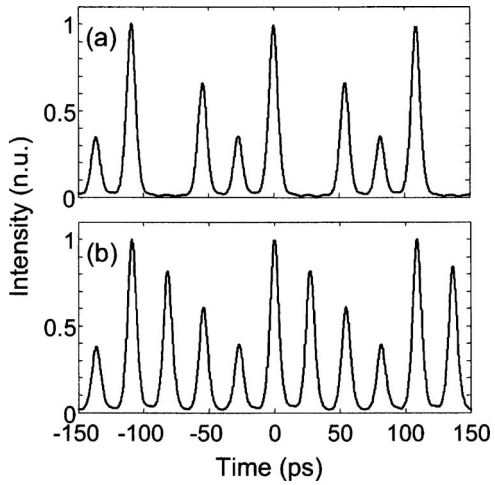

Fig. 6. Generation of arbitrary periodic pulse sequences. (a), (b) Measured intensity cross correlations of the pulse trains with peak-power patterns [1,0,2/3,1/3] and [1,0.8,0.6,0.4], respectively.

ditional periodic control on the relative peak power of the output pulses. The method is based on optimized periodic spectral filtering implemented via line-by-line pulse shaping. A wide variety of four-times multiplied periodic pulse sequences was successfully generated via phase-only line-by-line pulse shaping resulting in minimal power loss. In contrast, some sequences are generated with more fidelity when combined amplitude-and-phase periodic filtering is considered. Our experimental results show excellent agreement with the theoretical output pulse trains obtained with the optimized filters. Modulated pulse trains with higher multiplication factors can be readily achieved if input trains with shorter pulses are considered. This technique can also be implemented with other filtering setups with intrinsic periodic response such as, for example, 1D pulse shapers based on a virtually imaged phased array as a spatial disperser [20]. The line-by-line spectral shaping methods discussed here may also be implemented using integrated planar-lightwave-circuit-based pulse shapers, e.g., [21,22], provided that sufficient spectral resolution is available to permit high fidelity line-by-line control.

ACKNOWLEDGMENTS

This work was supported in part by the Defense Advanced Research Projects Agency/Air Force Office of Scientific Research under grant FA9550-06-1-0189 and by the National Science Foundation under grant ECCS-0601692. J. Caraquitena gratefully acknowledges a postdoctoral fellowship from the Ministerio de Educación y Ciencia, Spain.

REFERENCES

1. T. Sizer II, "Increase in laser repetition rate by spectral selection," IEEE J. Quantum Electron. **25**, 97–103 (1989).
2. P. Petropoulos, M. Ibsen, M. N. Zervas, and D. J. Richardson, "Generation of a 40-GHz pulse stream by pulse multiplication with a sampled fiber Bragg grating," Opt. Lett. **25**, 521–523 (2000).
3. K. Yiannopoulos, K. Vyrsokinos, E. Kehayas, N. Pleros, K. Vlachos, H. Avramopoulos, and G. Guekos, "Rate multiplication by double-passing Fabry–Perot filtering," IEEE Photon. Technol. Lett. **15**, 1294–1296 (2003).
4. K. Yiannopoulos, K. Vyrsokinos, N. Pleros, D. Tsiokos, C. Bintjas, G. Guekos, and H. Avramopoulos, "Repetition rate upgrade for optical sources," IEEE Photon. Technol. Lett. **15**, 861–863 (2003).
5. J. Azaña and M. A. Muriel, "Temporal self-imaging effects: theory and application for multiplying pulse repetition rates," IEEE J. Sel. Top. Quantum Electron. **7**, 728–744 (2001).
6. S. Arahira, S. Kutsuzawa, Y. Matsui, D. Kunimatsu, and Y. Ogawa, "Repetition-frequency multiplication of mode-locked pulses using fiber dispersion," J. Lightwave Technol. **16**, 405–410 (1998).
7. I. Shake, H. Takara, S. Kawanishi, and M. Saruwatari, "High-repetition-rate optical pulse generation by using chirped optical pulses," Electron. Lett. **34**, 792–793 (1998).
8. S. Longhi, M. Marano, P. Laporta, O. Svelto, M. Belmonte, B. Agogliati, L. Arcangeli, V. Pruneri, M. N. Zervas, and M. Ibsen, "40-GHz pulse-train generation at 1.5 μm with a chirped fiber grating as a frequency multiplier," Opt. Lett. **25**, 1481–1483 (2000).
9. J. Caraquitena, Z. Jiang, D. E. Leaird, and A. M. Weiner, "Tunable pulse repetition-rate multiplication using phase-only line-by-line pulse shaping," Opt. Lett. **32**, 716–718 (2007).
10. S. Kawanishi, "Ultrahigh-speed optical time-division-multiplexed transmission technology based on optical signal processing," IEEE J. Quantum Electron. **34**, 2064–2079 (1998).
11. J. D. McKinney, D. S. Seo, D. E. Leaird, and A. M. Weiner, "Photonically assisted generation of arbitrary millimeter-wave and microwave electromagnetic waveforms via direct space-to-time optical pulse shaping," J. Lightwave Technol. **21**, 3020–3028 (2003).
12. B. Xia and L. R. Chen, "A direct temporal domain approach for pulse-repetition rate multiplication with arbitrary envelope shaping," IEEE J. Sel. Top. Quantum Electron. **11**, 165–172 (2005).
13. B. Xia, L. R. Chen, P. Dumais, and C. L. Callender, "Ultrafast pulse train generation with binary code patterns using planar lightwave circuits," Electron. Lett. **42**, 1119–1120 (2006).
14. A. M. Weiner, "Femtosecond pulse shaping using spatial light modulators," Rev. Sci. Instrum. **71**, 1929–1960 (2000).
15. M. Mitchell, *An Introduction to Genetic Algorithms* (MIT Press, 1996).
16. F. G. Omenetto, B. P. Luce, and A. J. Taylor, "Genetic algorithm pulse shaping for optimum femtosecond propagation in optical fibers," J. Opt. Soc. Am. B **16**, 2005–2009 (1999).
17. F. G. Omenetto, A. J. Taylor, M. D. Moores, and D. H. Reitze, "Adaptive control of femtosecond pulse propagation in optical fibers," Opt. Lett. **26**, 938–940 (2001).
18. E. Zeek, R. Bartels, M. M. Murnane, H. C. Kapteyn, S. Backus, and G. Vdovin, "Adaptive pulse compression for transform-limited 15-fs high-energy pulse generation," Opt. Lett. **25**, 587–589 (2000).
19. Z. Jiang, D. E. Leaird, and A. M. Weiner, "Line-by-line pulse shaping control for optical arbitrary waveform generation," Opt. Express **13**, 10431–10439 (2005).
20. G. H. Lee and A. M. Weiner, "Programmable optical pulse burst manipulation using a virtually imaged phased array (VIPA) based Fourier transform pulse shaper," J. Lightwave Technol. **23**, 3916–3923 (2005).
21. D. Miyamoto, K. Mandai, T. Kurokawa, S. Takeda, T. Shioda, and H. Tsuda, "Waveform-controllable optical pulse generation using an optical pulse synthesizer," IEEE Photon. Technol. Lett. **18**, 721–723 (2006).
22. N. K. Fontaine, R. P. Scott, J. Cao, A. Karalar, W. Jiang, K. Okamoto, J. P. Heritage, B. H. Kolner, and S. J. B. Yoo, "32 phase × 32 amplitude optical arbitrary waveform generation," Opt. Lett. **32**, 865–867 (2007).